

## QED AND THE GROUND STATE OF HELIUM

W. HOGERVORST, K.S.E. EIKEMA, W. VASSEN and W. UBACHS  
*Laser Centre Vrije Universiteit, Department of Physics and Astronomy,  
De Boelelaan 1081, 1081 HV Amsterdam, The Netherlands*

With a phase-modulated extreme ultraviolet pulsed laser source the frequency of the  $1^1S - 2^1P$  transition of helium at 58 nm has been measured with high accuracy. The phase modulation scheme enabled measurement and reduction of frequency chirp, usually limiting the precision in pulsed spectroscopy. From the measured transition frequency of 5130495083(45) MHz of  $^4\text{He}$  a value of the ground state Lamb shift of 41224(45) MHz is deduced, in good agreement with a theoretical value of 41233(35) MHz based on QED calculations up to order  $\alpha^5 Z^6$ . Also an accurate value for the transition isotope shift  $^4\text{He} - ^3\text{He}$  of 263410(7) MHz has been determined.

### I Introduction

For many years one-electron systems like hydrogen [1] and positronium [2] were the only atomic systems in which low-energy quantum electrodynamic theory (QED) could be accurately tested. Progress in theoretical calculations also make multi-electron atoms and ions of interest for QED studies. Energy calculations without QED and higher-order relativistic effects in e.g. helium and helium-like ions are nowadays so accurate that experimental transition frequencies can be used as a test for Lamb shift calculations [3]. The most important contributions to the Lamb shift are the self-energy and vacuum polarization. Helium is particularly interesting because of two-electron contributions to the Lamb shift. They originate from mutual shielding of the nucleus by the electrons, decreasing the one-electron QED shift, and from a proximity effect of both electrons. Accurate measurements of the Lamb shift in helium are now available for the metastable  $2^{1,3}S$  states [4-7]. Two-electron Lamb shift contributions are best studied in  $^1S$  states where the proximity effect (self-energy) is ten times larger than in  $^3S$  states, contributing up to 10% to the total Lamb shift [3]. Experimental values for the  $2^1S$  Lamb shift were deduced from high resolution cw laser spectroscopy on transitions to  $1snp$  [4-6] and  $1snd$  states [7] by Drake et al. [8], in reasonable agreement with their theoretical calculations. Recently Shiner et al. [9] measured the isotope shift  $^4\text{He} - ^3\text{He}$  in the transition  $2^3S_1 - 2^3P_0$  with high precision, from which an accurate value for the nuclear charge radius of  $^3\text{He}$  could be extracted.

The Lamb shift in the  $1^1S$  ground state as well as its two-electron contribution are more than one order of magnitude larger than in the  $2^1S$  state. Also isotope shifts in ground state transitions are largest. However, the ground state is not easily accessible due to the large energy difference with excited states. In 1993 we showed in a preliminary experiment on the  $1^1S - 2^1P$  transition at 58.4 nm that this energy difference can be bridged using high power pulsed laser systems and harmonic up-conversion [10]. This encouraged us to start a dedicated experiment using a CW laser at 584 nm and pulse amplification techniques. However, precision spectroscopy with such a pulsed laser system is hampered by unwanted phase modulation effects in pulse-dye-amplifiers (PDA). Phase modulation results in time-dependent frequency excursions (chirp) which lead to a calibration error for the pulsed output relative to the frequency standards based on cw laser saturation spectroscopy in the visible. This effect turned out to be the limiting uncertainty in this experiment. We recently obtained a  $1^1S$  Lamb shift of 41260(175) MHz and measured the isotope shift  $^4\text{He} - ^3\text{He}$  to be 263410(7) MHz [11]. This latter value is more than two orders of magnitude better than the classical value of Herzberg [12] and is not sensitive to chirp effects. The early experiments on e.g. hydrogen encountered similar problems, before cw excitation was eventually achieved [see Ref. 13]. Many experiments, however, can at present only be performed by pulsed excitation. As a result the study of frequency chirp has become an active field of research. Heterodyning techniques have been developed to measure chirp phenomena [14,15] and methods to decrease chirp, such as anti-chirping of excimer-laser driven systems (pulse length 20-30 ns), were investigated [16].

Here we present a precision measurement of the  $1^1S - 2^1P$  transition of helium at 58 nm using phase-modulated narrow band extreme ultraviolet radiation (XUV). A fast electro-optic modulator (EOM) system was employed to control the phase (chirp) of a PDA at 584 nm which provides the power for non-linear upconversion to 58.4 nm. Together with an accurate chirp measurement technique for nanosecond pulses and precise modelling of the excitation process, we demonstrate that frequency chirp can be reduced significantly.

## 2 Experiment

A schematic of the setup is shown in Fig.1. The principle of the measurement is described elsewhere [11]. A PDA, pumped by an injection-seeded Nd:YAG laser (10 Hz, 740 mJ at 532 nm in a 6.5 ns pulse), amplifies 150 mW of light at 584 nm from a

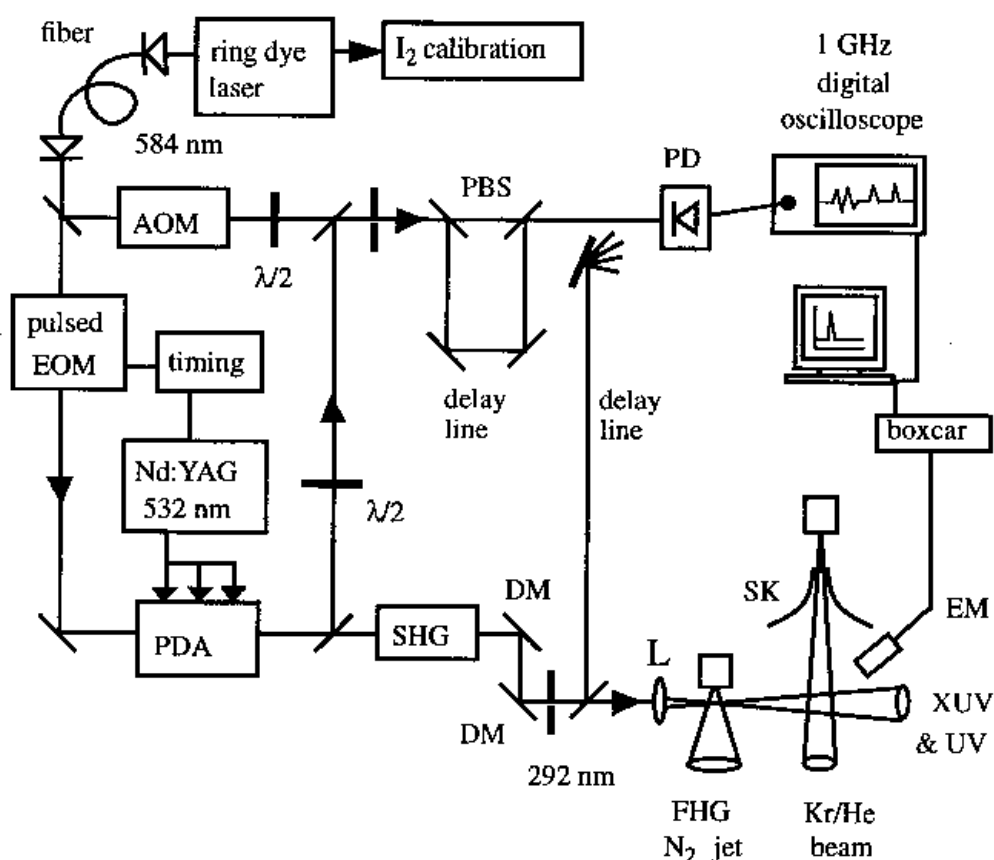


Fig. 1 : Schematic of the experimental setup (AOM=acousto-optic modulator, EOM=electro-optic modulator, PBS=polarizing beamsplitters, PDA=pulse dye amplifier, DM=dichroic mirror, FHG=fifth harmonic generation, PD=photodiode, SK=skimmer, EM=electron multiplier)

ring dye laser to 220 mJ in 6.5 ns pulses. This output is frequency doubled in a KD\*P crystal to  $\sim 100$  mJ at 292 nm in a 6 ns pulse, and subsequently focused ( $f=24.3$  cm) in a pulsed jet of  $N_2$  for fifth-harmonic generation. In this process  $10^5$ - $10^6$  photons at 58.4 nm are generated in a beam overlapping with the UV. To reduce Doppler effects the  $1^1S - 2^1P$  transition is induced in a skimmed and pulsed beam ( $\sim 18$  mrad divergence) of 10% helium seeded in 90% krypton. The seeding slows down helium atoms to 480(100) m/s compared to 1200(300) ms for pure helium. A few percent of the atoms excited to  $2^1P$  state is ionized by the UV light. A pulsed extraction field is used to collect and detect the ions with an electron multiplier and boxcar integrator. The primary calibration is performed at 584 nm by saturation spectroscopy on the

P88(15-1)-o transition in  $I_2$  [11]. Additional tests of pressure- and light shifts improved calibration of this transition to 513049427.1(1.7) MHz, leading to an uncertainty of 17 MHz in the XUV.

### 3 Chirp measurement and compensation

Frequency deviations (chirp) in the PDA output relative to the cw laser seed beam is a result of phase modulation due to time-dependent gain in the amplification process [see Ref. 15]. To modify or counteract this chirp a  $LiTaO_3$  EOM was developed to modulate the phase of the cw seed beam prior to amplification in the PDA. By apply-

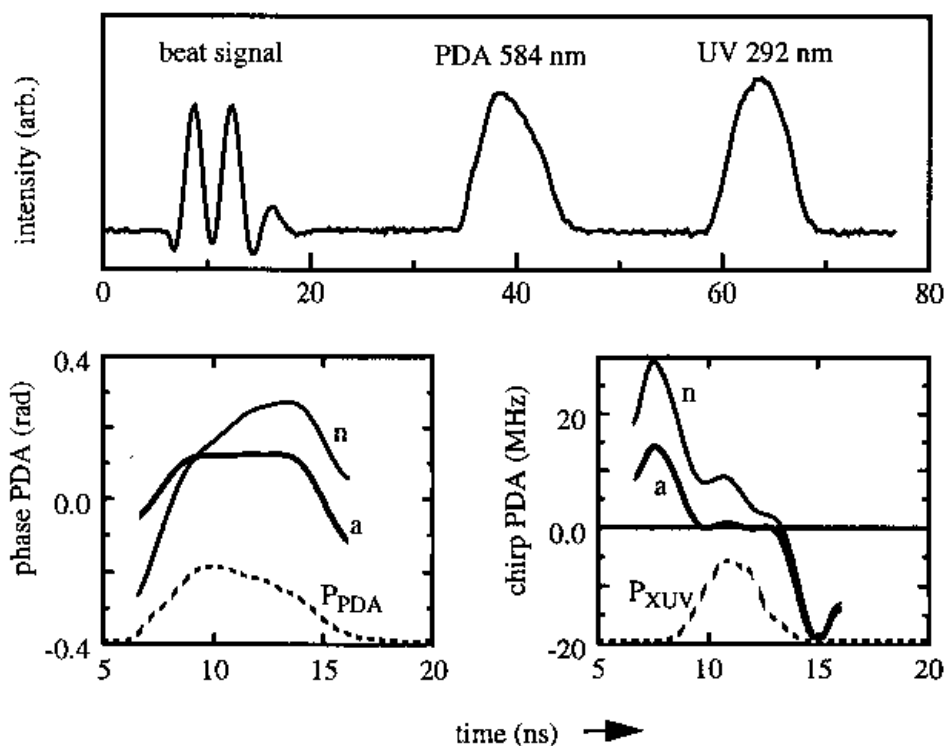


Fig. 2: Chirp measurement of normal (n) and anti-chirped (a) PDA pulses (average over 10 pulses). Upper part: typical oscilloscope readout with beat signal between PDA output and 250 MHz frequency shifted cw beam, the PDA pulse and UV pulse. Lower part: phase changes and resulting frequency chirp in the PDA. Dotted lines represent the PDA and XUV pulse shape ( $P_{XUV} \sim P_{UV}^{4.5}$ ). Under conditions of anti-chirp the reconstructed phase is constant and the frequency excursion close to zero during the time window of XUV-generation.

ing a pulsed driving voltage to the EOM the average frequency chirp can be either decreased or increased by varying the width and slope of the rising and falling edge. The total phase modulation is monitored with a method similar to that of Fee et al.[14] by heterodyning part of the PDA output with the cw seed beam, 250 MHz acousto-optically shifted (see Fig. 1). We extended this method by measuring also the (time-delayed) PDA and UV pulse on the same photodiode connected to a 1 GHz bandwidth, 5 Gs/s digital oscilloscope. A perpendicular polarization component is used to measure the PDA pulse intensity at exactly the same position in the beam where the heterodyne signal is observed. With this information the heterodyne signal can be corrected for the effects of the pulse envelope, resulting in accurate phase reconstruction even for short pulses of 6.5 nanosecond duration. The phase  $\Phi$  and chirp  $\Delta\nu = (1/2\pi) d\Phi/dt$  of the PDA pulses (see Fig. 2) is monitored on line together with an estimate of the expected frequency shift effect in the XUV. In this manner the chirp can be adjusted interactively with the EOM. Most of the chirp measurements are based on an average of 50–100 laser pulses to reduce the influence of pulse to pulse chirp fluctuations of about 1–10 MHz.

From the measured dependence of the ion signal on UV power (ion signal  $\sim P_{uv}^{5.5}$ ) it follows that chirp compensation with the EOM is only necessary in the central part of the PDA pulse (Fig. 2). However, processes such as ionization of the non-linear medium may shift XUV generation to the leading edge of the UV pulse. To get a better understanding of the effect of chirp on the resonance transition we also performed measurements with induced chirp. For this purpose a 2 ns wide chirp pulse of  $\sim 80$  MHz is applied with different time delays relative to the PDA output pulse. In the XUV this results in rapid frequency sweeps of  $\sim 800$  MHz. In each case the spectrum of the  $1^1S - 2^1P$  transition is recorded, together with a chirp measurement in the visible (averaging over 100 laser pulses). From the chirp measurements, the simultaneously recorded UV pulses, and the measured dependence of the ion signal on UV power a predicted spectrum based on numerical integration of the optical Bloch equations is calculated. Comparison with the experimental lineshapes in Fig. 3 shows that the effect of chirp on the  $1^1S - 2^1P$  is well understood. Due to the intense short additional chirp pulses the transition lineshape (asymmetry and linewidth) is highly sensitive to the effective XUV production timing. As a result the XUV production time window could be set accurately at  $+0.2(4)$  ns relative to the UV pulse centre, with a XUV pulse width of  $\sim 3(0.5)$  ns. We conclude that XUV is indeed produced only at the peak UV intensity, so chirp reduction is necessary only in the centre of the PDA pulse. This is accomplished by applying a counteracting phase modulation to the PDA seed beam ('anti-chirp'), resulting in a flat phase and considerably reduced

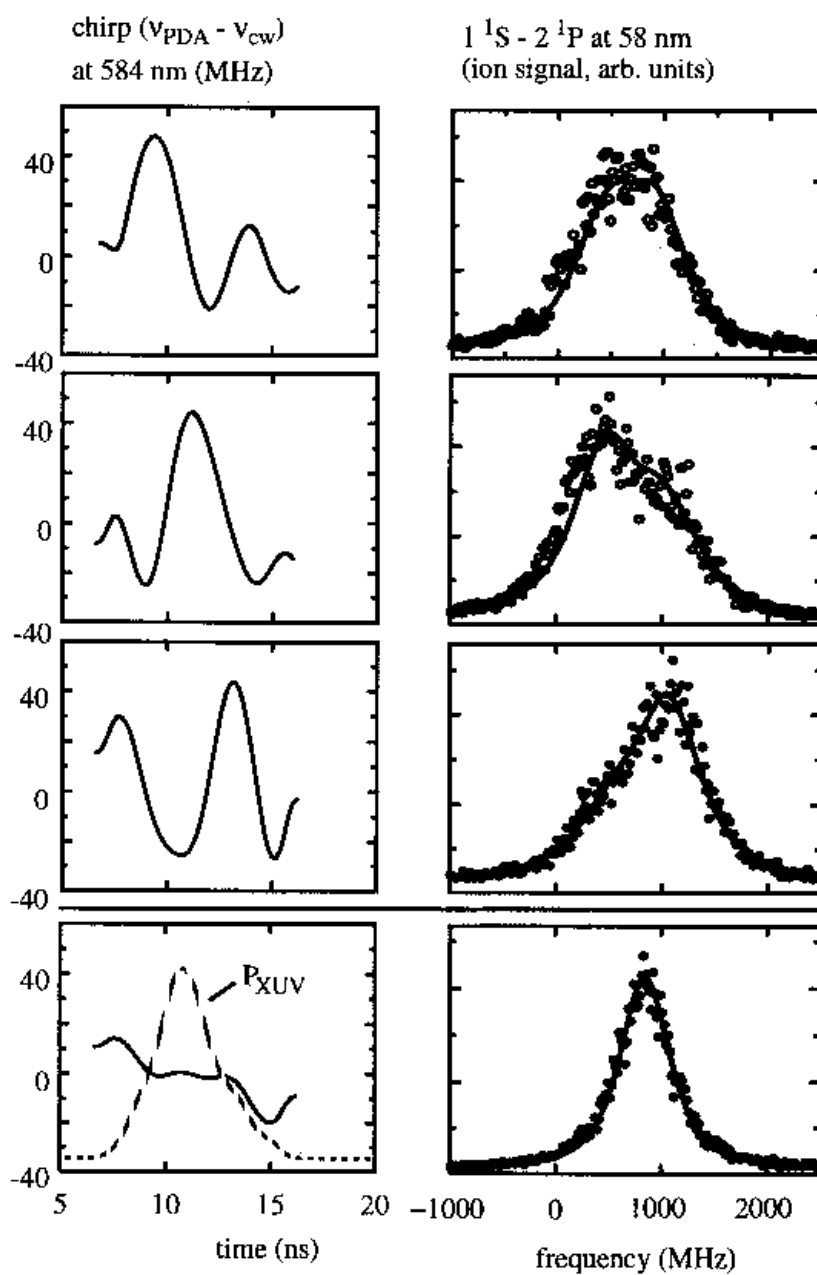


Fig. 3: Dependence of experimental and calculated  $1\ ^1S - 2\ ^1P$  transition lineshape (right side, average over 4 scans) on chirp (left side, average over 100 laser pulses). The upper three traces show the distortion due to extra chirp, while the lower trace shows a typical 'anti-chirped' lineshape. The origin is the position of the  $I_2$  calibration. The dotted line in the 'anti-chirped' measurement is the estimated XUV power dependence on UV power.

Table 1: Experimental and theoretical values for the  $1^1S - 2^1P$  transition frequency with their  $1\sigma$  errors. All numbers in MHz.

	value	$1\sigma$
Measured, (PDA chirp corrected)	5130495110	5
Corrections:		
Chirp : measurement analysis	*	14
PDA beam inhomogenities	-	20
5th harmonic, measured	10	13
Dynamic Stark shift	-44	15
Doppler shift	7	20
drift ( <i>systematic</i> )	-	3
Line shape	-	3
I <sub>2</sub> calibration	-	17
Corrected value; experimental	5130495083	45
Theory	5130495074	35
* : already included in 'measured'		

chirp in the time window of interest (Fig. 2). Applying such anti-chirp the resonance frequency shifts 65 - 90 MHz upward, but no change in resonance line shape is observed due to the relatively small 'normal' chirp excursions. Calculated residual chirp shift is typically  $< 10$  MHz, for which the measurements were corrected. The difference between calculated and measured anti-chirp shift is always within 10 MHz, determined for a large part by the statistical uncertainty in the XUV transition measurements. The uncertainty in the exact timing and width of the XUV pulse and in the chirp measurement procedure itself generates an uncertainty in the calculated anti-chirp of 14 MHz. Variation of the chirp over the spatial profile of the PDA beam was measured as well, resulting in an additional uncertainty of 20 MHz in the XUV (see Table 1).

At the UV power density used for fifth-harmonic generation ( $< 10^{13}$  W/cm<sup>2</sup>) frequency chirp may also arise from ionization/excitation and time-dependent UV field-induced refractive index changes in the gaseous nonlinear medium. The ionization/excitation effect has been measured by changing the N<sub>2</sub> density in two UV focal power density situations, resulting in a small correction of +10(13) MHz. The UV field-induced chirp is a single-atom effect and can not be measured by changing the

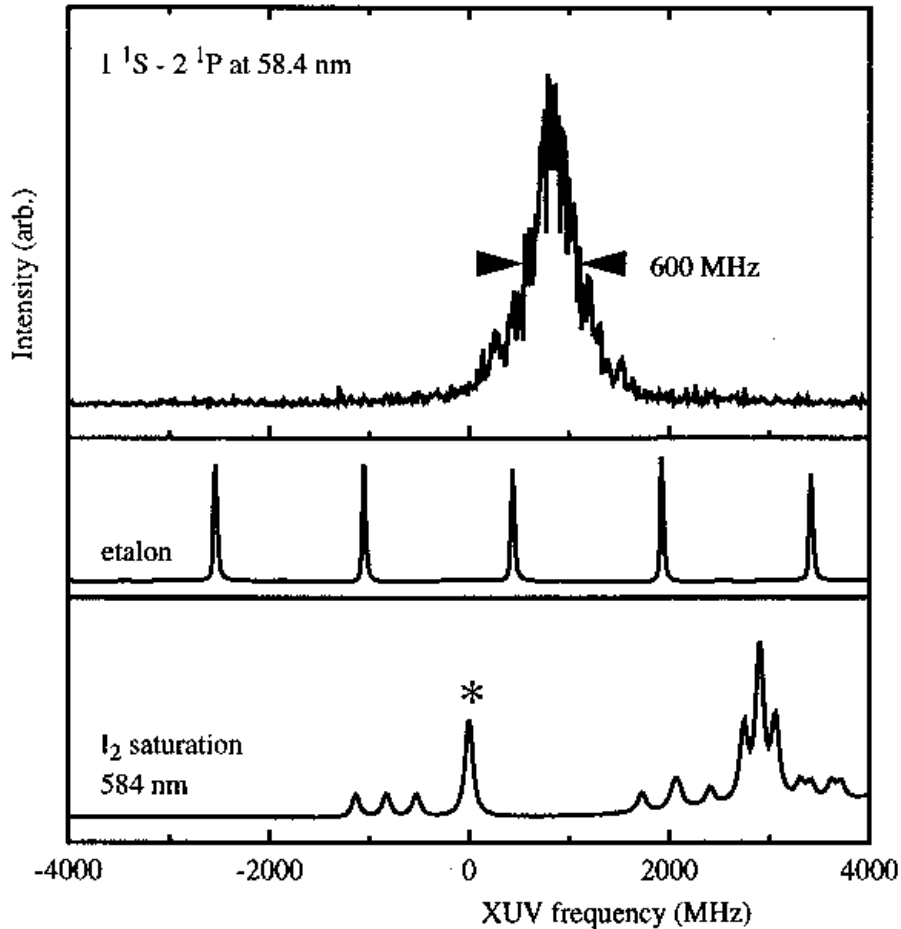


Fig. 4: The  $1\ ^1S - 2\ ^1P$  resonance transition for anti-chirped PDA pulses with etalon and  $I_2$  saturated absorption spectrum. The \* indicates the 'o'-component of the P88(15-1) transition used for absolute calibration.

density of the  $N_2$ . Due to the increased interest in high-harmonic generation also estimates for this effect are now available [17], which show that the average effect is negligible in our case. The same can be concluded for frequency-doubling-induced chirp in KD\*P. This follows from a comparison of a recent realistic calculation [18] with our visible power density of  $\sim 72\ \text{MW}/\text{cm}^2$  and an estimated maximum phase mismatch of  $\Delta k = 0.07\ \text{mm}^{-1}$ . The additional chirp from self-phase modulation in KD\*P [19] is even smaller. The uncertainty of these small effects are correlated (due to XUV production timing) and are included in the chirp correction uncertainty of 14 MHz.

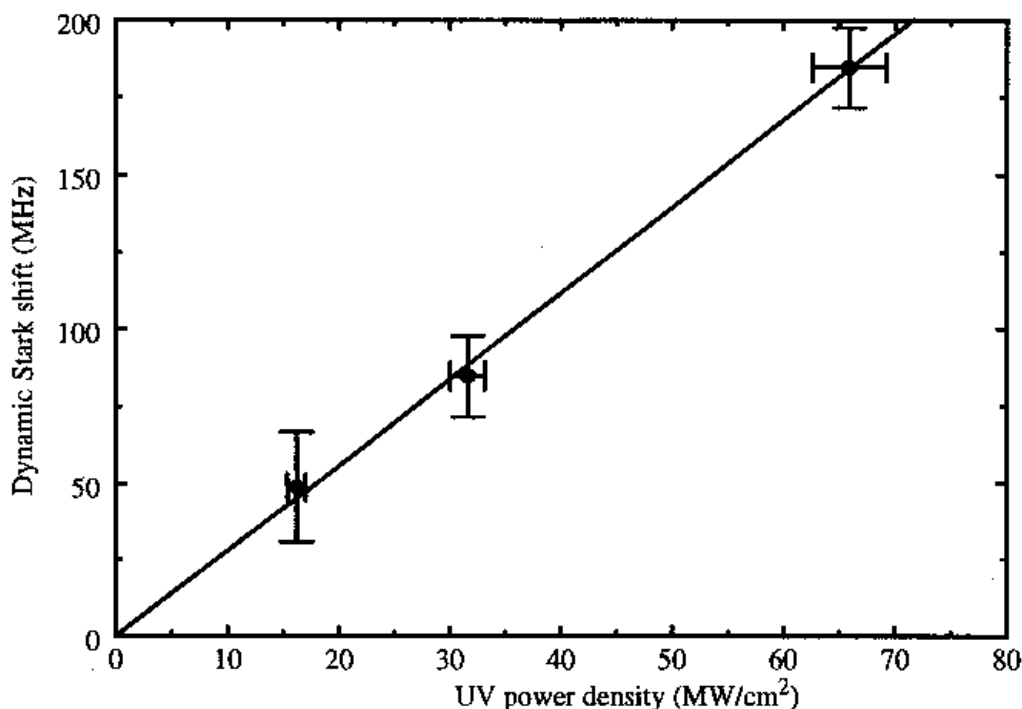


Fig. 5: Dynamic Stark shift measurement in  $^4\text{He}$  as a function of UV power density in the interaction region. The horizontal error bars indicate the uncertainty in the relative UV power densities. The absolute UV power has an accuracy of 40-50 %.

#### 4 Results

For the final measurement first a Doppler shift of  $-7(20)$  MHz was determined from a number of recordings with the He/Kr mixture and with pure helium, all under 'normal' chirp conditions. This was followed by scans with anti-chirped XUV. An example of a scan under anti-chirp conditions is shown in Fig. 4. Included is a saturated absorption spectrum of the relevant iodine line as well as an etalon spectrum. The  $1^1\text{S} - 2^1\text{P}$  average transition frequency of  $5130495110(5)$  was determined from a weighted average of all normal-chirp and anti-chirped measurements. A small frequency drift with time (attributed to beam alignment changes) introduced a systematic uncertainty of 3 MHz. In our recent experiment [11] backscatter from the skimmer disturbed the atomic beam resulting in a Doppler-broadened asymmetric transition line shape of 950 MHz. With a new skimmer a symmetric transition lineshape of  $\sim 600$  MHz (natural linewidth is 300 MHz) is now obtained. The uncertainty in the

determination of the line centre due to the resonance lineshape is 3 MHz.

The influence of dynamic Stark shift on the  $1\ ^1S - 2\ ^1P$  transition due to the high UV intensity (previously calculated to be  $3.1\ \text{Hz}/\text{Wcm}^{-2}$  [11]) was addressed by measuring the resonance position in quick succession with three pre-aligned lenses (24.3 cm, 33.9 and 49.0 cm) used to focus the UV for harmonic generation. This procedure changes the UV power density in the detection region from  $\sim 16\ \text{MW}/\text{cm}^2$  for the 24.3 cm lens to  $\sim 66\ \text{MW}/\text{cm}^2$  for the 49.0 cm lens. The expected strong reduction in XUV power due to decreasing UV power in the focus is largely compensated by improved phase-matching and increased ionization rate. Linear extrapolation of the resonance frequency to zero UV power (Fig.5) yields a dynamic Stark shift of 44(15) MHz for the 24.3 cm lens used in the final measurements, in good agreement with calculations.

Our final value for the  $1\ ^1S - 2\ ^1P$  transition frequency is 5130495083(45) MHz (Table 1), in excellent agreement with the value published earlier [see ref. 11] but four times more accurate. The theoretical value is 5130495074(35) MHz, consisting of a non-QED part that is known with high accuracy, a  $1\ ^1S$  Lamb shift contribution of  $-41233$  MHz (including terms of order  $\alpha^5 Z^6$  and 2-loop corrections) and a  $2\ ^1P$  Lamb shift contribution of  $-37.5$  (1.8) MHz [3,8]. The error in the theoretical  $1\ ^1S$  Lamb shift is entirely due to terms of order  $\alpha^5 Z^6$ . In a  $1/Z$  expansion only the leading term,  $-68.8$  MHz, has been calculated. Higher-order terms are therefore estimated to be smaller by a factor of 2, resulting in a theoretical uncertainty estimate of 35 MHz. The theoretical uncertainty in the  $2\ ^1P$  level is only 1.8 MHz and therefore not important. As a result an improved ionization potential of He of 198310.6672(15)  $\text{cm}^{-1}$  can be deduced. The good agreement between the theoretical Lamb shift of 41233(35) MHz and the experimental value of 41224(45) MHz may be interpreted as a verification of the approximation used to calculate a two-electron relativistic contribution of 771.11 MHz of order  $\alpha^4 Z^5$  for which no full theory exists. A similar agreement was found for the  $2\ ^1S$  level in helium [8] and the  $2\ ^3S$  level in  $\text{Li}^+$  [20]. With this experiment we achieved an unprecedented accuracy of 9 parts in  $10^9$  in XUV spectroscopy. It provides an experimental test of QED-phenomena in the ground state of helium at the accuracy level of present day calculations.

### Acknowledgements

We wish to thank G.W.F. Drake for making available unpublished calculations and for useful comments, and acknowledge financial support of the Netherlands Foundation for Fundamental Research on Matter (FOM).

## References

1. M. Weitz, A. Huber, F. Schmidt-Kaler, D. Leibfried, W. Vassen, C. Zimmermann, K. Pachucki, T.W. Hänsch, L. Julien, F. Biraben, *Phys. Rev. A* **52**, 2664 (1995)
2. K.P. Jungmann in *Atomic Physics* 14, p102; Eds D.J. Wineland, C.E. Wieman and S.J. Smith (American Institute of Physics, 1995).
3. G.W.F. Drake, *Adv. At. Mol. Opt. Phys.* **31**, 1 - 62 (1993) , and private communication with G.W.F. Drake. See also: G.W.F. Drake in *Atomic Physics* 13, p3; Eds. H. Walther, T.W. Hänsch and B. Neizert (American Institute of Physics, 1993).
4. D. Shiner, R. Dixon, P. Zhao, *Phys. Rev. Lett.* **72**, 1802 (1994).
5. F.S. Pavone, F. Marin, P. DeNatale, M. Inguscio, F. Biraben, *Phys. Rev. Lett.* **73**, 42 (1994). See also M. Inguscio *et al.* in *Atomic Physics* 14, p81; Eds D.J. Wineland, C.E. Wieman and S.J. Smith (American Institute of Physics, 1995).
6. C. J. Sansonetti and J.D. Gillaspay, *Phys. Rev. A* **45**, R1 (1992).
7. W. Lichten, D. Shiner, Z. X. Zhou, *Phys. Rev. A* **43**, 1663 (1991).
8. G.W.F. Drake, I.B. Khriplovich, A.I. Milstein, A.S. Yelkhovsky, *Phys. Rev. A* **48**, R15 (1993).
9. D. Shiner, R. Dixon and V. Vedantham, *Phys. Rev. Lett.* **74**, 3553 (1995).
10. K.S.E. Eikema, W. Ubachs, W. Vassen, and W. Hogervorst, *Phys. Rev. Lett.* **71**, 1690 (1993).
11. K.S.E. Eikema, W. Ubachs, W. Vassen, and W. Hogervorst, *Phys. Rev. Lett.* **76**, 1216 (1996).
12. G. Herzberg, *Proc. Roy. Soc. London A* **248**, 309 (1958).
13. C. Wieman and T.W. Hänsch, *Phys. Rev. A* **22**, 192 (1980).
14. M.S. Fee, K. Danzmann, S. Chu, *Phys. Rev. A* **45**, 4911 (1992).
15. N. Melikechi, S. Gangopadhyay, and E.E. Eyler, *J. Opt. Soc. Am. B* **11**, 2402 (1994).
16. I. Reinhard, M. Gabrysch, B. Fischer van Weikersthal, K. Jungmann and G. zu Putlitz, *Appl. Phys. B*. accepted for publication.
17. M. Lewenstein, P. Salières, A. L'Huillier, *Phys. Rev. A* **52**, 4747 (1995).
18. A.V. Smith, M.S. Bowers, *J. Opt. Soc. Am. B* **12**, 49 (1995).
19. R. Adair, L.L. Chase, S. A. Payne, *Phys. Rev. B* **39**, 3337 (1989).
20. E. Riis, A.G. Sinclair, O. Poulsen, G.W.F. Drake, W.R.C. Rowley, and A.P. Levick, *Phys. Rev. A* **49**, 207 (1994).